J. Fluid Mech. (1992), *vol.* 237, *pp.* 57–71
Printed in Great Britain

Fixed-flux convection in a tilted slot

By PAOLA CESSI† AND W. R. YOUNG
Scripps Institution of Oceanography, University of California at San Diego,
La Jolla, CA 92093, USA

(Received 26 November 1990 and in revised form 10 September 1991)

We study fixed-flux convection in a long, narrow slot which is inclined to the horizontal. (Gravity is in the vertical direction, and horizontal is perpendicular to this.) Because of the fixed-flux boundary conditions the convective modes have much larger lengthscales in the along-slot direction than in the transverse direction. In the case of a horizontal slot this disparity in scales has been previously exploited to obtain an amplitude equation for the single mode which first becomes unstable as the Rayleigh number is increased above critical. When the slot is tilted we show that there is a distinguished limit in which there are two active modes in the slightly supercritical regime. This new limit is when the horizontal wavenumber, the supercriticality, and the tilt of the slot away from vertical, are all small. A modification of the well-known expansion for fixed flux convection in a horizontal slot leads to a coupled system of partial differential equations for the amplitudes of the two modes.

Numerical solution of this system suggests that all initial conditions eventually evolve into one of the two states, both of which consist of a single, steady roll in the cavity. The states are distinguished by the direction of circulation of the roll, and by the buoyancy fields, which are quite different in the two cases.

1. Introduction and background

Convection between poorly conducting boundaries, through which a flux of buoyant contaminant is imposed, has been recognized as an analytic avenue into a strongly nonlinear regime. Remarkable simplifications are possible because the most unstable modes have large horizontal lengthscales relative to the depth of the layer. Thus the vertical structure of the dynamical variables, such as buoyancy and stream function, can be explicitly calculated while the evolution of the horizontal structure is obtained from a derived amplitude equation. The prototypical example is that of Chapman & Proctor (1980) in which a Boussinesq fluid convects between horizontal surfaces. The implications of this model for convection in the Earth's mantle are discussed by Chapman, Childress & Proctor (1980).

Other examples in which the extreme aspect ratio of the convective modes can be exploited include mildly penetrative convection (Roberts 1985), non-Boussinesq convection (Depassier & Spiegel 1982), and bioconvection (Childress & Spiegel 1992).

In all of the works we have mentioned the surfaces which confine the fluid are horizontal and gravity is normal to them. The result of the expansion is a partial differential equation of the form

$$f_t = -f_{xx} - f_{xxxx} + (f_x^2 + f^2)_{xx} + (f_x^3)_x + \ldots, \tag{1.1}$$

† Permanent address: Istituto FISBAT-CNR, Bologna, Italy.

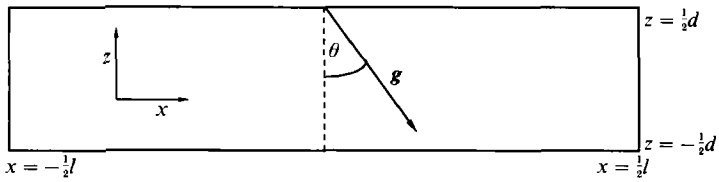

FIGURE 1. Definition sketch of the geometry of the tilted slot. The slot is horizontal when $\theta = 0$ and vertical when $\theta = \frac{1}{2}\pi$.

where we indicated the most important terms up to third order in f. The quadratic terms in (1.1) result from breaking of the Boussinesq symmetry by temperature-dependent material properties, mixed boundary conditions, nonlinearity in the equation of state, etc. $f(x,t)$ is the amplitude of the mode which becomes linearly unstable when the critical Rayleigh number is exceeded.

In this article we discuss the consequences of tilting the layer of fluid relative to the gravity vector, $\boldsymbol{g}$. The geometry is illustrated in figure 1 where we suppose that $\boldsymbol{z}\cdot\boldsymbol{g} = -g\cos\theta$. In all of our earlier references the slot is horizontal so that $\theta = 0$. In a study of thermohaline planform selection Proctor & Holyer (1986) studied the complementary case of perfectly vertical cells ($\theta = \frac{1}{2}\pi$). We find that there is a distinguished limit when θ is very close to $\frac{1}{2}\pi$, so that the slot is almost vertical. As in the earlier study of Proctor & Holyer (1986) there is more than one active mode. In our case the analogue of (1.1) is a system of two coupled partial differential equations for the modal amplitudes. When $\theta = \frac{1}{2}\pi$ the system reduces to a special case of the multimode description given by Proctor & Holyer (1986). We recover (1.1) as a special case of our system when the departure of θ from $\frac{1}{2}\pi$ becomes large, and one of the two modes becomes very stable. The purpose of the present work is to clarify the role of slight departures from a perfectly vertical geometry and so to present a unified framework which describes single-component fixed-flux convection in large-aspect-ratio containers.

The expansion described below captures the qualitative features of several other examples of convection in narrow inclined slots. For example Phillips (1970) discusses steady convective motion in an inclined liquid-filled fissure. In this example motion is sustained because there is a buoyancy flux in the x-direction, i.e. along the axis of the fissure. The problem of a perfectly horizontal cavity ($\theta = 0$), again forced by a flux in the x-direction, has been discussed in detail by Cormack, Leal & Imberger (1974*a*), Cormack, Leal & Seinfeld (1974*b*) and Imberger (1974). These examples motivate an additional geometric complication which is not indicated in figure 1: we allow the direction of the externally imposed flux to be at an angle θ' to the vertical. When $\theta = \theta'$ (e.g. Chapman & Proctor 1980 where both of these angles are zero or Proctor & Holyer 1986 where they are both $\frac{1}{2}\pi$) there is a motionless conductive state which becomes unstable when a critical Rayleigh number is exceeded. However, if these two angles are unequal, as in Phillips (1970), then convection occurs at zero Rayleigh number. In the expansion below we clarify this point by showing that there is a forcing parameter, β, proportional to $\theta - \theta'$, in the amplitude equations (2.29).

Because of its geophysical importance, fixed-flux convection in tilted fluid layers has also been discussed in the context of porous media (Lapwood convection). Riley & Winters (1990) is a recent study with a thorough review of the literature on Lapwood convection. Because Riley & Winters restrict attention to a square cavity their results (numerical solutions of the unreduced partial differential equations) are not directly comparable to the present work which uses an aspect-ratio expansion to

obtain the amplitude equations in (2.29). However, Sen, Vasseur & Robillard (1988) and Linz (1990) use the Darcy resistance law in the momentum equations and the 'parallel flow approximation' to obtain analytic solutions in the central portion of an inclined cavity. The parallel flow approximation is similar in spirit to the approach of Phillips (1970) and Cormack *et al.* (1974*a*). In these works it is assumed that the axial lengthscale is infinite so that the velocity is strictly unidirectional and varies only in the cross-channel direction. The numerical solutions of Sen *et al.* (1988) show that this is appropriate in the middle of the cavity, where the influence of the endwalls is negligible. The aspect-ratio expansion developed here includes this approximation as a special case: here the variations along the axis of the channel have a finite lengthscale which is much greater than the depth of the cavity. The parallel flow approximation corresponds to the steady solution of (1.1) in which f_x is a constant. (This requires that the non-Boussinesq term $(f^2)_{xx}$ be absent.)

2. The expansion

We consider a layer of Boussinesq fluid contained in a slot of depth d and length l. The aspect ratio is

$$\epsilon \equiv d/l, \tag{2.1}$$

and we suppose that this non-dimensional parameter is very small: $\epsilon \ll 1$. The coordinates are Cartesian with $-\frac{1}{2}d < z < \frac{1}{2}d$ and $-\frac{1}{2}l < x < \frac{1}{2}l$. The gravity vector is

$$\boldsymbol{g} = g(\sin\theta \boldsymbol{x} - \cos\theta \boldsymbol{z}), \tag{2.2}$$

where $\boldsymbol{x}$ and $\boldsymbol{z}$ are unit vectors in the x- and z-directions. When $\theta = 0$ the slot is horizontal and when $\theta = \frac{1}{2}\pi$ the slot is vertical.

The density of the fluid is represented as

$$\rho = \rho_0(1 - g^{-1}\mathscr{B}), \tag{2.3}$$

where $\mathscr{B}$ is the buoyancy. External sources of buoyancy impose a constant flux through the layer and we suppose that the flux vector is directed at an angle θ' to the vertical. Thus the buoyancy can be written as

$$\mathscr{B} = \Gamma(\sin\theta' x - \cos\theta' z) + b, \tag{2.4}$$

where $\Gamma(\sin\theta' x - \cos\theta' z)$ is the basic state stratification and b is the buoyancy perturbation produced by motion of the fluid. The basic state stratification in (2.4) satisfies the boundary conditions on the normal derivative of $\mathscr{B}$ required by the externally imposed flux. Thus the boundary condition on the field induced by the motion of the fluid, b, is

$$\kappa \nabla b \cdot \boldsymbol{n} = 0, \tag{2.5}$$

where κ is the diffusivity of buoyancy and $\boldsymbol{n}$ is the unit normal to the walls of the cavity.

The motion is assumed to be two-dimensional, so that we can use a stream function

$$u = \psi_z, \quad w = -\psi_x, \quad \zeta \equiv \nabla^2\psi = -\nabla \times \boldsymbol{u} \cdot \boldsymbol{y}, \tag{2.6}$$

and write the vorticity equation as

$$\zeta_t + u\zeta_x + w\zeta_z = \nu\nabla^2\zeta - \sin\theta b_z - \cos\theta b_x + \Gamma\sin(\theta - \theta'), \tag{2.7}$$

where ν is the viscosity. The buoyancy equation is

$$b_t + u(\Gamma\sin\theta' + b_x) + w(-\Gamma\cos\theta' + b_z) = \kappa\nabla^2 b. \tag{2.8}$$

If the buoyancy flux is parallel to gravity, so that $\theta = \theta'$, then there is a conductive solution of (2.7) and (2.8), i.e. $\psi = b = 0$. This motionless state becomes unstable to convection when the externally imposed buoyancy gradient, Γ, exceeds a critical value. In Chapman & Proctor (1980), $\theta = \theta' = 0$ and in Proctor & Holyer (1986), $\theta = \theta' = \frac{1}{2}\pi$.

When $\theta \neq \theta'$ there is no conductive solution and small external buoyancy sources produce convection. In Cormack *et al.* (1974*a*, *b*), and Imberger (1974) the slot is horizontal ($\theta = 0$), and the flux is perpendicular to gravity so that $\theta' = \frac{1}{2}\pi$. In Elder (1965) the slot is vertical ($\theta = \frac{1}{2}\pi$), and again the flux is perpendicular to gravity so that in this case $\theta' = 0$. (Elder used fixed temperature, rather than fixed flux, so that the following analysis does not apply directly to his configuration.)

2.1. *Non-dimensional variables and the distinguished limit*

Convenient non-dimensional variables are

$$x = l\hat{x}, \quad z = d\hat{z}, \quad t = (l^2/\kappa)\hat{t}, \quad \psi = \epsilon\kappa\hat{\psi}, \quad b = \epsilon d\Gamma\hat{b}. \tag{2.9}$$

Dropping the hats, the non-dimensional equations of motion are

$$Pr^{-1}\epsilon^2(\zeta_t + \psi_z\zeta_x - \psi_x\zeta_x) = \nabla^2\zeta - \sin\theta Rab_z - \epsilon\cos\theta Rab_x + \epsilon^{-1}\sin(\theta-\theta')Ra, \tag{2.10a}$$

$$\epsilon^2(b_t + \psi_z b_x - \psi_x b_z) = -\sin\theta\psi_z - \epsilon\cos\theta\psi_x + \nabla^2 b, \tag{2.10b}$$

where $\nabla^2 = \epsilon^2\partial_x^2 + \partial_z^2$ and $\zeta = \epsilon^2\psi_{xx} + \psi_{zz}$. The five non-dimensional parameters are the angles, θ and θ', the aspect ratio in (2.1), and the Rayleigh and Prandtl numbers

$$Ra \equiv \frac{d^4\Gamma}{\nu\kappa}, \quad Pr \equiv \frac{\nu}{\kappa}. \tag{2.11}$$

The expansion we use below is in powers of ϵ^2:

$$(\psi, b) = (\psi_0, b_0) + \epsilon^2(\psi_2, b_2) + \ldots \tag{2.12}$$

and is based on the distinguished limit $\theta \to \frac{1}{2}\pi$ and $\theta' \to \theta$, as $\epsilon \to 0$. We introduce

$$\chi \equiv \epsilon^{-1}\cos\theta \quad \text{and} \quad \phi \equiv \epsilon^{-3}\sin(\theta-\theta')Ra \tag{2.13}$$

into (2.10), and fix χ and ϕ while $\epsilon \to 0$. Thus the expansion pivots around the configuration in which the slot is vertical ($\theta = \frac{1}{2}\pi$) and the bottom endwall ($x = \frac{1}{2}l$ in figure 1) is heated with constant flux, while the upper endwall ($x = -\frac{1}{2}l$ in figure 1) is cooled to the same rate so that the net amount of heat in the fluid does not change. Thus the heat flux is also vertical ($\theta' = \frac{1}{2}\pi$). To recover this purely vertical configuration one takes $\chi = \phi = 0$ in the following expansion.

When $\phi = 0$ there is a conductive basic state which becomes unstable to convection when $Ra > R_0$. The unknown critical Rayleigh number, R_0, will emerge as the expansion unfolds. We suppose that the Rayleigh number differs slightly from the critical value and define R_2 by

$$Ra = R_0 + \epsilon^2 R_2. \tag{2.14}$$

With this new notation the vorticity equation is

$$\begin{aligned} Pr^{-1}\epsilon^2(\partial_t + \partial_z\psi_0\,\partial_x - \partial_x\psi_0\,\partial_z)\partial_z^2\psi_0 &= (\partial_z^4 + 2\epsilon^2\partial_z^2\partial_x^2)(\psi_0 + \epsilon^2\psi_2) \\ &\quad - [1 - \epsilon^2(\tfrac{1}{2}\chi^2)](R_0 + \epsilon^2 R_2)\partial_z(b_0 + \epsilon^2 b_2) - \epsilon^2\chi R_0\,\partial_x b_0 + \epsilon^2\phi, \end{aligned} \tag{2.15}$$

where terms of order ϵ^4 have been suppressed. We find below that the amplitude

equations emerge at ϵ^2 (i.e. at the second level in the expansion) so that these terms are not needed. Likewise the buoyancy equation is

$$\epsilon^2(\partial_t+\partial_z\psi_0\partial_z-\partial_x\psi_0\partial_z)b_0=-[1-\epsilon^2(\tfrac{1}{2}\chi^2)]\partial_z(\psi_0+\epsilon^2\psi_2)$$
$$-\epsilon^2\chi\partial_x\psi_0+(\partial_z^2+\epsilon^2\partial_x^2)(b_0+\epsilon^2 b_2). \quad (2.16)$$

2.2. *The zero-order solution*

Collecting the terms of order ϵ^0 we have the system

$$\left.\begin{aligned}\partial_z^4\psi_0-R_0\partial_z b_0&=0,\\ \partial_z^2 b_0-\partial_z\psi_0&=0.\end{aligned}\right\} \quad (2.17)$$

Because the boundary conditions at $z=\pm\frac{1}{2}$ are $\partial_z b_0=\psi_0=0$ one can easily integrate the second equation and then substitution gives a fourth-order boundary-value problem for ψ_0. We write the solution in the form

$$\psi_0=\tilde{A}(x,t)F(z) \quad \text{and} \quad b_0=\tilde{A}(x,t)G(z)+\tilde{B}(x,t) \quad (2.18)$$

where $\tilde{A}(x,t)$ and $\tilde{B}(x,t)$ are amplitudes whose evolution is determined at next order. The shape functions, $F(z)$ and $G(z)$, and the critical Rayleigh number, R^0, are obtained by solving the eigenvalue problem

$$F^{\mathrm{iv}}-R_0F=0 \quad \text{and} \quad G'=F. \quad (2.19)$$

The boundary conditions are no normal flow through the walls of the channel

$$F(\pm\tfrac{1}{2})=0, \quad (2.20)$$

and one of the three possibilities: (*a*) slip: $F''(\pm\frac{1}{2})=0$; (*b*) no slip: $F'(\pm\frac{1}{2})=0$; (*c*) mixed: $F'(-\frac{1}{2})=F''(\frac{1}{2})=0$. To specify a unique solution of (2.19) and (2.20) we also require the normalization

$$\overline{F^2}=1 \quad \text{and} \quad \bar{G}=0, \quad (2.21)$$

where the overbar denotes an average over the depth of the fluid

$$\bar{f}\equiv\int_{-\frac{1}{2}}^{\frac{1}{2}}f\,\mathrm{d}z. \quad (2.22)$$

The simplest choice of boundary condition is case (*a*) so that $R_0=\pi^4$, $F=\sqrt{2}\cos(\pi z)$ and $G(z)=(\sqrt{2}/\pi)\sin(\pi z)$. The two other cases are given in Appendix A.

The leading-order solution in (2.18) is a linear superposition of two modes, $\tilde{A}$ and $\tilde{B}$. This distinguishes the present expansion from that of Chapman & Proctor (1980) and Normand (1984). Chapman & Proctor's single-mode amplitude equation will be contained as a special case ($\chi\to\infty$) in which limit the $\tilde{A}$ mode is 'slaved' to the $\tilde{B}$ mode. Normand did not include the $\tilde{B}$ mode in the leading-order solution and consequently did not obtain the correct amplitude equation. In fact we find that with both modes in (2.18) the nonlinearity is quadratic and a consistent system is obtained at next order, ϵ^4. With only the $\tilde{A}$ mode one finds an amplitude equation with a cubic nonlinearity at order ϵ^6.

2.3. *The first-order solution and the solvability condition*

At next order, ϵ^2, one has

$$\partial_z^4\psi_2-R_0\partial_z b_2=Pr^{-1}[\tilde{A}_tF''+\tilde{A}\tilde{A}_xH']-2\tilde{A}_{xx}F''$$
$$+[R_2-(\tfrac{1}{2}\chi^2)R_0]\tilde{A}F+\chi R_0(\tilde{A}_xG+\tilde{B}_x)-\phi, \quad (2.23a)$$

$$\partial_z^2 b_2-\partial_z\psi_2=\tilde{A}_tG+\tilde{A}\tilde{A}_xJ+\tilde{B}_t+\tilde{A}\tilde{B}_xF'-(\tfrac{1}{2}\chi^2)\tilde{A}F'$$
$$+\chi\tilde{A}_xF-\tilde{A}_{xx}G-\tilde{B}_{xx}, \quad (2.23b)$$

where we have introduced

$$H \equiv F'^2 - FF'' \quad \text{and} \quad J \equiv F'G - G'F. \tag{2.24}$$

The solvability condition for the B mode is simply the vertical integral of (2.23b). Noting that $\bar{J} = -2$ gives us the first amplitude equation:

$$\tilde{B}_t = -\chi \bar{F} \tilde{A}_x + \tilde{B}_{xx} + (\tilde{A}^2)_x. \tag{2.25}$$

The solvability condition for the $\tilde{A}$ mode is obtained by multiplying (2.23a) by F and (2.23b) by G. Averaging over z, and then eliminating $\overline{F\,\partial_z b_2}$, gives the second amplitude equation:

$$\begin{aligned}[R_0 \overline{G^2} + Pr^{-1}\overline{F'^2}]\tilde{A}_t = {} & [R_2 - \chi^2 R_0]\tilde{A} + [2\overline{F'^2} + R_0 \overline{G^2}]\tilde{A}_{xx} \\ & + R_0 \chi \bar{F} \tilde{B}_x + R_0 \tilde{A}\tilde{B}_x + [Pr^{-1}\overline{FH'} - R_0 \overline{GJ}]\tilde{A}\tilde{A}_x - \bar{F}\phi. \end{aligned} \tag{2.26}$$

2.4. *The canonical form of the amplitude equations*

We now put the amplitude equations in a canonical form using some cosmetic rescaling,

$$\tilde{A} = \alpha A \quad \text{and} \quad \tilde{B} = \alpha^2 B, \tag{2.27}$$

where

$$\alpha \equiv (2R_0^{-1}\overline{F'^2} + \overline{G^2})^{\frac{1}{2}}. \tag{2.28}$$

In terms of these rescaled variables we have

$$pA_t = rA + cB_x + A_{xx} + AB_x + \gamma(A^2)_x - \beta, \tag{2.29a}$$

$$B_t = -cA_x + B_{xx} + (A^2)_x, \tag{2.29b}$$

where the coefficients are

$$\left.\begin{aligned} p \equiv \frac{Pr^{-1}\overline{F'^2} + R_0 \overline{G^2}}{R_0 \alpha^2}, \quad r \equiv \frac{R_2 - \chi^2 R_0}{R_0 \alpha^2}, \quad c \equiv \frac{\chi \bar{F}}{\alpha}, \\ \gamma \equiv -\frac{Pr^{-1}\overline{F'H} + R_0 \overline{GJ}}{2R_0 \alpha}, \quad \beta \equiv \frac{\bar{F}\phi}{R_0 \alpha^3}. \end{aligned}\right\} \tag{2.30}$$

Equation (2.29) is the final form of our amplitude equations. In Appendix A we have summarized the calculation of the five coefficients, p, r, c, γ and β, for the three sets of boundary conditions. In the next section we discuss some limiting cases of the system in (2.29).

To conclude this section we state the boundary conditions applied to (2.29). To avoid a detailed analysis of flow near the endwalls we adopt

$$A(\pm\tfrac{1}{2}) = 0 \quad \text{and} \quad B_x(\pm\tfrac{1}{2}) = 0. \tag{2.31}$$

We give a heuristic justification for this choice by noting that with the boundary conditions in (2.31) the integral of (2.29b) over the length of the slot is

$$\partial_t \int_{-\frac{1}{2}}^{\frac{1}{2}} B \, \mathrm{d}x = 0. \tag{2.32}$$

Thus the integral of the leading-order buoyancy perturbation, b_0 in (2.18), over the area of the slot is constant in time, and this is consistent with the exact no-flux condition in (2.5). Also the requirement $A(\pm\frac{1}{2}) = 0$ ensures that the leading-order approximation to the stream function, ψ_0, satisfies the condition of no mass flux through the endwalls.

3. Properties of the amplitude equations

3.1. *The linear problem*

We begin our analysis of the amplitude equations in (2.29) with a discussion of the unforced ($\beta = 0$), associated linear problem

$$\left.\begin{aligned} pA_t &= rA + cB_x + A_{xx}, \\ B_t &= -cA_x + B_{xx}. \end{aligned}\right\} \tag{3.1}$$

Substituting $[A, B] = [\hat{A}, \hat{B}] \exp(ikx + st)$ gives the dispersion relation

$$ps^2 + [(1+p)k^2 - r]s + k^4 - k^2(c^2 + r) = 0. \tag{3.2}$$

For the moment we ignore the boundary conditions at $x = \pm\frac{1}{2}$ and suppose that k is a continuous variable.

The structure of the roots is summarized in figure 2. We fix c and p and decrease r, starting with $r > c^2$ in panel (a) of figure 1 and concluding with $r = -c^2$ in panel (f). Fixing c and p is equivalent to fixing the Prandtl number, Pr, and the tilt, θ. Decreasing r is then accomplished by decreasing Ra. Thus in the parameter plane shown in figure 3 we are descending along the vertical line and the points labelled (a–f) on this curve correspond to the dispersion curves in the various parts of figure 2.

Figure 2(a) shows that when $r > c^2$ the most unstable wavenumber is $k = 0$. In addition there is a stable branch which is, however, neutral at $k = 0$. In figure 2(b, c) we show that as r decreases below c^2 the most unstable wavenumber moves away from $k = 0$ while there is no change in the structure of the stable branch. When $r \leqslant 0$ (figures 2d and 2e) there is an important change in the configuration of the branches. The unstable branch now passes through the origin, $(k, s) = (0, 0)$, while the stable branch is now damped rather than neutral at $k = 0$. Finally, in figure 2f, when $r \leqslant -c^2$, the instability disappears.

In the parameter plane of figure 3 there are two important landmarks indicated by the solid curves. First there is the stability boundary, $r = -c^2$ which passes through point (f). Using the results from Appendix A for slip boundary conditions, this curve is

$$Ra = \pi^4 + (\pi^4 - 8\pi^2)\cos^2\theta. \tag{3.3}$$

The almost coincident dashed curve is the result of an exact calculation of the stability boundary (see Appendix B). There is excellent agreement between the approximation and the exact result even when $\theta = 0$.

The second landmark in the parameter plane is the curve on which there is the exchange of modal identity shown in figure 2(d). This is the solid curve in figure 3 which passes through point (d). On this curve $r = 0$, or for slip boundary conditions,

$$Ra = \pi^4(1 + \cos^2\theta). \tag{3.4}$$

Once again, an exact calculation of this curve is given in Appendix B (the result is $Ra = \pi^4/\sin^2\theta$) and is shown as dashed in figure 3.

Now in the finite domain, $-\frac{1}{2} < x < \frac{1}{2}$, the wavenumber is quantized, i.e. $k = n\pi$, where $n = 1, 2$, etc. If the gravest mode, $k = \pi$, falls within the interval of instability in figure 2 then the conductive solution, $A = B = 0$, is unstable. In fact there is a supercritical pitchfork bifurcation from each unstable mode. In the next subsection we discuss the finite-amplitude development of these instabilities.

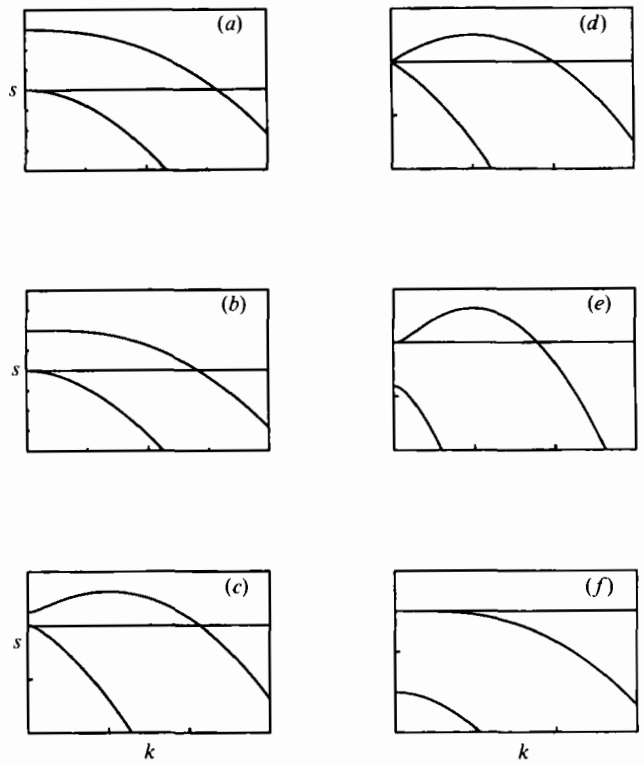

FIGURE 2. Summary of the solution of the linear stability problem for the system of amplitude equations in (2.29). (*a*) $r > c^2$, (*b*) $r = c^2$, (*c*) $r < c^2$, (*d*) $r = 0$, (*e*) $-c^2 < r < 0$, (*f*) $r = -c^2$.

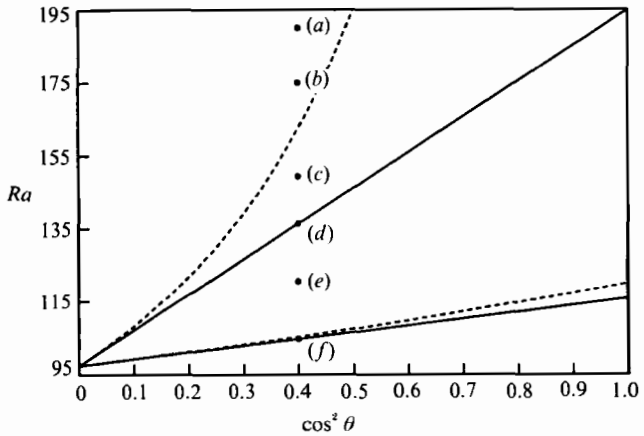

FIGURE 3. This figure shows the (Ra, θ) parameter plane and a comparison of the approximate critical Rayleigh numbers (solid curves) with their exact counterparts (dashed curves) for stress-free boundary conditions. Our expansion pivots about the point $Ra = \pi^4$ and $\cos^2\theta = 0$ where the two Rayleigh-number curves intersect and the approximate curves are tangent to the exact curves. (*a*–*f*) correspond to parts (*a*–*f*) of figure 2.

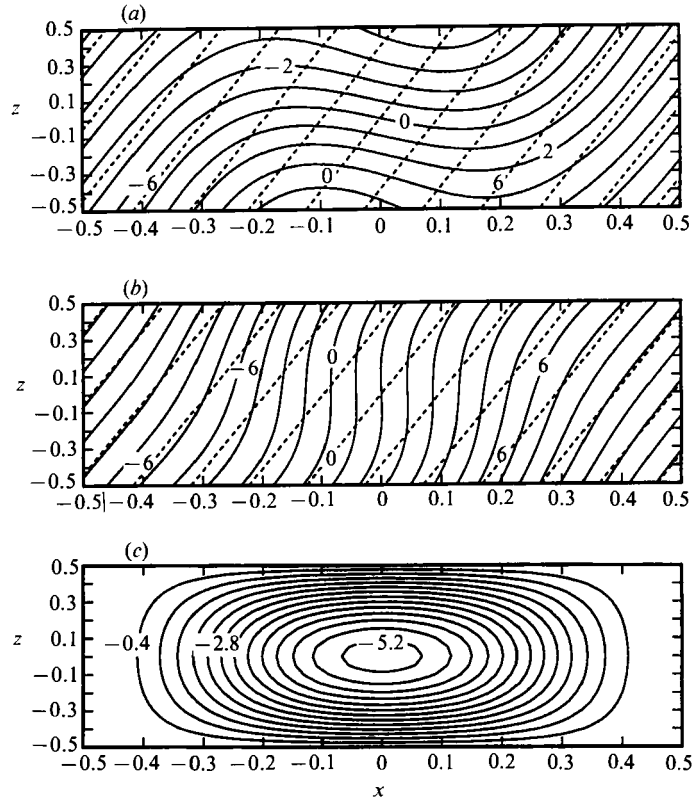

FIGURE 4. Two steady solutions of the amplitude equations (2.29) with $r = 0$, $c = 4.6$, $p = 1$, $\gamma = 0$, and $\beta = 0$. In (*a*) and (*b*) we show the two-dimensional fields for the total (solid line) and unperturbed (dashed line) buoyancy. We only show the stream-function field, (*c*), for the 'direct' circulation because the other state corresponds to the reversed circulation. The two-dimensional fields have been reconstructed using $d/l = 0.25$, $\theta = \frac{1}{4}\pi$ and vertical modes appropriate to no-stress boundary conditions.

3.2. *Steady-state solutions*

We now turn to the steady nonlinear solutions of the amplitude equations:

$$0 = B_{xx} - (cA - A^2)_x, \tag{3.5a}$$

$$0 = A_{xx} + rA + (c + A)B_x + \gamma(A^2)_x - \beta. \tag{3.5b}$$

Integrating (3.5*a*) we obtain

$$A_{xx} + (r + c^2)A - A^3 + \gamma(A^2)_x - \beta = 0, \tag{3.6a}$$

$$B_x = cA - A^2. \tag{3.6b}$$

Thus A satisfies an equation which is identical to that in Chapman & Proctor (1980) (apart from the external forcing represented by β). The further analytic reduction of (3.6*a*) is described in that reference.

Two solutions of (3.6) are shown in figure 4. Here we have taken $c = 4.6$, $\gamma = \beta = r = 0$ and solved (2.29) by time stepping with $p = 1$. We then took $\epsilon = 0.25$ and $\theta = \frac{1}{4}\pi$ and reconstructed the leading-order approximations to the stream function and buoyancy fields using (2.18) with the F and G appropriate to slip

boundary conditions. (We selected these extreme values of the perturbation parameter values for visual clarity in figure 4.)

Both the solutions in figure 4 are grave modes (i.e. $A(x)$ has no internal zeros). Some initial conditions evolve into a steady solution with $A > 0$, while others fall into the steady solution with $A < 0$, and the two solutions differ by a change in sign of A. (Note that when $\gamma = \beta = 0$ if $A(x)$ is a solution of (3.6a) then so is $-A(x)$.) All of the initial conditions we tried eventually reached one of these two steady states and we speculate that these are global attractors for the amplitude equations in (2.29). Thus, with the parameters in figure 4, although there are steady solutions with more structure (i.e. A has internal zeros) the numerical evidence suggests that these are unstable to larger-scale perturbations. And there was no evidence of sustained time dependence, such as limit cycles or chaos.

We emphasize that there are two distinct grave modes in figure 4. Although the two A are related by $A(x) = -A(x)$, when $c \neq 0$ the B are very different in both structure and amplitude. This point is emphasized in figure 4 where we plotted one of the two stream functions, but both of the buoyancy fields. The buoyancy field in figure 4(c) is 'anomalous' in the sense that the corresponding stream function (with $A(x) > 0$) consists of a counterclockwise circulation in the tilted slot. This means that on the lower sidewall of the slot ($z = -\frac{1}{2}d$) the buoyant fluid is carried downwards, in the direction of gravity, by the circulation. Analogous 'indirect' circulation patterns have been reported in tilted Lapwood convection by Sen *et al.* (1988) and Riley & Winters (1990).

Figure 4 shows that the two grave steady solutions have very different buoyancy fields because the amplitude of B is very different in the two cases. But this visual presentation conceals some underlying similarities between the two flows. For instance, the buoyancy gradient parallel to gravity, expressed in terms of A and B, is

$$\mathscr{G}(x,z) \equiv \boldsymbol{g}\cdot\boldsymbol{\nabla}\mathscr{B} = g\Gamma[1+\epsilon^2\alpha(\alpha B_x + A_x G - \chi F A) + O(\epsilon^4)]. \tag{3.7}$$

For steady solutions we use (3.6b) to write B_x in terms of A. If (3.7) is then averaged across the channel one finds

$$\bar{\mathscr{G}}(x) = \frac{1}{d}\int_{-d/2}^{d/2} \boldsymbol{g}\cdot\boldsymbol{\nabla}\mathscr{B}\,\mathrm{d}z = g\Gamma(1-\epsilon^2\alpha^2A^2 + O(\epsilon^4)). \tag{3.8}$$

Thus, after averaging across the channel, the destabilizing buoyancy distribution which drives convection is the same for the two grave solutions.

Evolution towards one of the two grave solutions seems to be a general property of the amplitude equations in (2.29). We integrated (2.29) with $\beta = 0, 0.1 \leqslant p \leqslant 2$, $-20 \leqslant r \leqslant 80, 0 \leqslant c \leqslant 15, 0 \leqslant \gamma \leqslant 7$, and found that grave solutions, of the type shown in figure 4, are attractors for all the initial conditions we tried. Thus, despite its complicated appearance, the system (2.29) exhibits a very simple behaviour in the long-time limit. We do not have an analytic proof of this assertion but in the next two subsections we discuss special cases in which the system can be reduced equations which are known to be generated by Lyapunov functionals.

We have also done some computations with non-zero β. Once again we find that the system always evolves to a steady-stable solution in which A has no internal zeros. That is, the gravest modes are apparently universal attractors for all initial conditions no matter whether the system is forced ($\beta \neq 0$) or unforced ($\beta = 0$).

3.3. *Behaviour for large p*

If p is very large then B evolves on a much slower timescale than A and so falls into quasi-steady balance. Thus when $p \gg 1$ we adiabatically eliminate the B mode. With the aid of (3.6*b*) the evolution equation for A is then:

$$pA_t = A_{xx} + (r+c^2)A - A^3 + \gamma(A^2)_x. \tag{3.9}$$

If $\gamma = 0$ then (3.9) is the real Ginsburg–Landau equation and using the well-known variational argument one can show that all initial conditions eventually evolve into the gravest steady solutions. With the 'advective' term proportional to γ this reasoning fails and we have been unable to prove analytically that (3.9) always reaches a steady state. But extensive numerical calculations suggest that this is the case. We have integrated (3.9) varying $r+c^2$ from 0 to 200 and γ from 1 to 7, with various initial conditions. In every case the system evolved to a steady state with no internal zeros.

3.4. *Behaviour for large c*

If the tilt of the slot, represented by the parameter c, is very large then we recover the case analysed by Chapman & Proctor (1980). The system (2.29) reduces to a single equation describing the evolution of B. A further assumption is needed to be in the Chapman & Proctor limit: the most unstable mode must be only slightly supercritical and the Rayleigh number $r+c^2$ must be only slightly greater than zero so that as in figure 2(*e*) there is a damped mode. With these parameter restrictions in mind we introduce

$$\epsilon \equiv c^{-1} \ll 1, \quad \mu^2 \equiv r+c^2, \quad f \equiv \epsilon B, \quad \tau \equiv \epsilon^2 t. \tag{3.10}$$

Notice that with the new scaling B is of the same order as $c \gg 1$, while A and μ are $O(1)$. f and A now satisfy

$$\epsilon^4 pA_\tau = \epsilon^2 A_{xx} + (\epsilon^2\mu^2 - 1)A + f_x + \epsilon A f_x + \gamma\epsilon^2(A^2)_x - \epsilon^2\beta \tag{3.11a}$$

$$\epsilon^2 f_\tau = f_{xx} - A_x + \epsilon(A^2)_x. \tag{3.11b}$$

We now expand A and f in powers of ϵ

$$(A,f) = (A_0,f_0) + \epsilon(A_1,f_1) + \ldots \tag{3.12}$$

and find a single equation for $f_0(x,t)$ at $O(\epsilon^2)$. At order ϵ^0 (3.11*a*) and (3.11*b*) are both

$$A_0 = \partial_x f_0. \tag{3.13}$$

At next order, ϵ^1, (3.11*a*) and (3.11*b*) both give

$$A_1 = \partial_x(A_0^2) + \partial_x f_1, \tag{3.14}$$

and we can take $f_1 = 0$. The evolution equation for f_0 emerges at order ϵ^2, where

$$0 = \partial_x^2 A_0 + \mu^2 A_0 + \gamma\partial_x A_0^2 + A_1\partial_x f_0 - (A_2 - \partial_x f_2) - \beta, \tag{3.15a}$$

$$\partial_\tau f_0 = 2\partial_x(A_0 f_1) + \partial_x(\partial_x f_2 - A_2). \tag{3.15b}$$

Eliminating $\partial_x f_2 - A_2$ from (3.15*b*), and using (3.13) and (3.14) we finally have

$$\partial_\tau f_0 = -\mu^2\partial_x^2 f_0 - \partial_x^4 f_0 + \partial_x(\partial_x f_0)^3 - \gamma\partial_x^2(\partial_x f_0)^2, \tag{3.16}$$

which is the evolution equation of Chapman & Proctor (1980). When $\gamma = 0$ they prove that (3.16) always reaches a stable steady state which is the gravest mode. Chapman & Proctor's numerical integrations indicated that with $\gamma \neq 0$ a stable steady state is also reached.

3.5. *The case of a perfectly vertical slot*: $\beta = c = \gamma = 0$

In the case of a perfectly vertical slot with symmetric boundary conditions ($c = \beta = \gamma = 0$) the amplitude equations in (2.29) reduce to a special case of the system obtained by Proctor & Holyer (1986). In this study of thermohaline convection the extreme aspect ratio of the cells ('salt fingers') motivates an expansion which is very similar to the one presented here. Our case is obtained by suppressing the salinity mode, and retaining only one convection mode, in Proctor & Holyer's multi-mode system. Once again, our numerical solution indicates that (2.29) always approaches one of the two grave steady solutions of (3.5). But with $c = 0$ the buoyancy fields of these two solutions, calculated from (3.6), are identical.

4. Conclusion

We have shown how a double expansion, based on both small wavenumbers and small departures from $\theta = \frac{1}{2}\pi$, leads to a unified framework for describing convection driven by imposed fluxes of buoyancy. The resulting amplitude equations, (2.29), govern the evolution of the two modes which are active in this distinguished limit.

In certain parts of the parameter space one of the two modes evolves on a much faster timescale than the other and further analytic reduction is possible. For example, as the tilt increases, and the slot becomes closer to horizontal, we recover the well-known amplitude equation in (1.1), except for the term $\partial_x^2 f^2$. The missing term, which appears in Depassier & Spiegel (1982) and Roberts (1985), is due to strongly non-Boussinesq effects such as temperature-dependent viscosity. These have not been included in our analysis.

Numerical integration has led us to speculate that the system in (2.29) always evolves to one of the two gravest modes, i.e. eventually there is one convective cell which fills the box. This result has been presaged by Chapman & Proctor's numerical solution of (1.1) (without the term $\partial_x^2 f^2$) but we have been unable to prove that this is a general result.

P.C. was supported by the Italian National Research Council (CNR) and the National Science Fouundation. W.R.Y. was supported by the National Science Foundation and the Office of Naval Research. We thank Andrew Woods and Yves Pomeau for helpful discussion and FISBAT for hospitality during the preparation of this work.

Appendix A. Coefficients of the amplitude equations

In this appendix we summarize the calculation of the coefficients of the amplitude equations in (2.30). There are three cases depending on the choice of boundary condition.

We begin with the easiest case, which is slip: $F''(\pm\frac{1}{2}) = 0$. The solution of the eigenproblem in (2.19), (2.20) and (2.21) is

$$R_0 = \pi^4, \quad F = \sqrt{2}\cos(\pi z), \quad G = (\sqrt{2}/\pi)\sin(\pi z). \tag{A 1}$$

Thus $\bar{F} = 2\sqrt{2}/\pi$ and $\alpha = \sqrt{3}/\pi$. The coefficients in (2.30) are

$$p = \tfrac{1}{3}(1+Pr^{-1}), \quad r = \frac{Ra - \pi^4(1+\cos^2\theta)}{3\pi^2\epsilon^2}, \quad c = \frac{4\cos\theta}{\epsilon\sqrt{6}}, \quad \beta = \frac{(\frac{2}{3})^{\frac{3}{2}}\sin(\theta-\theta')Ra}{\pi^2\epsilon^3}. \tag{A 2}$$

γ is zero because the eigenfunctions are symmetric about the middle of the slot.

Turning now to no slip, the solution of the eigenproblem is in Chandresakhar (1961, appendix v). The critical Rayleigh number is

$$R_0 \equiv \lambda^4 = (4.730\,040\,74)^4, \tag{A 3}$$

where λ is the smallest positive solution of $\tanh(\frac{1}{2}\lambda) + \tan(\frac{1}{2}\lambda) = 0$. The eigenfunctions are

$$F = \frac{\cosh(\lambda z)}{\cosh(\frac{1}{2}\lambda)} - \frac{\cos(\lambda z)}{\cos(\frac{1}{2}\lambda)}, \quad G = \frac{1}{\lambda}\left[\frac{\sinh(\lambda z)}{\cosh(\frac{1}{2}\lambda)} - \frac{\sin(\lambda z)}{\cos(\frac{1}{2}\lambda)}\right], \tag{A 4}$$

and after some algebra and numerical evaluation we find $\bar{F} = 0.8309$, $R_0\bar{G} = 49.4812$ and $\overline{F'^2} = 12.3026$. With the results above it is easy to numerically evaluate the expressions for the coefficients in (2.28) and (2.30). However, there is a simple approximation which leads to concise expressions. To within a few per cent $\lambda \approx \frac{3}{2}\pi$, $\bar{F} \approx 8/3\pi$, $\overline{F'^2} \approx 4\pi$ and $R_0\overline{G^2} \approx 16\pi$. Using these approximations one finds $\alpha \approx (128/27\pi^3)^{\frac{1}{2}}$ and from the definitions in (2.30):

$$\left.\begin{aligned} p \approx \tfrac{1}{6}(Pr^{-1}+4), \quad r \approx \frac{Ra-(\frac{3}{2}\pi)^4(1+\cos^2\theta)}{24\pi\epsilon^2}, \quad c \approx \frac{(\frac{3}{2}\pi/2)^{\frac{1}{2}}\cos\theta}{\epsilon}, \\ \beta \approx \frac{(\frac{3}{2}\pi)^{\frac{1}{2}}\sin(\theta-\theta')\,Ra}{24\pi\epsilon^3}. \end{aligned}\right\} \tag{A 5}$$

Once again, γ is zero because the eigenfunctions are symmetric about the middle of the slot.

The final case is mixed boundary conditions in which there is no slip, $F'(-\frac{1}{2}) = 0$, on the lower plate and slip, $F''(\frac{1}{2}) = 0$, on the upper plate. The eigenfunctions are

$$\left.\begin{aligned} F = \frac{1}{2}\left[\frac{\cosh(\mu z)}{\cosh(\frac{1}{2}\mu)} - \frac{\cos(\mu z)}{\cos(\frac{1}{2}\mu)} + \frac{\sin(\mu z)}{\sin(\frac{1}{2}\mu)} - \frac{\sinh(\mu z)}{\sinh(\frac{1}{2}\mu)}\right], \\ G = \frac{1}{2\mu}\left[\frac{\sinh(\mu z)}{\cosh(\frac{1}{2}\mu)} - \frac{\sin(\mu z)}{\cos(\frac{1}{2}\mu)} - \frac{\cos(\mu z)}{\sin(\frac{1}{2}\mu)} - \frac{\cosh(\mu z)}{\sinh(\frac{1}{2}\mu)} + \frac{4}{\mu}\right], \end{aligned}\right\} \tag{A 6}$$

where

$$R_0 \equiv \mu^4 = (3.926\,602\,31)^4. \tag{A 7}$$

μ is the smallest positive solution of the $\tan\mu = \tanh\mu$. After some algebra and numerical evaluation we find $\bar{F} = 0.8600$, $R_0\overline{G^2} = 23.2311$ and $\overline{F'^2} = 11.5125$. In this asymptotic case γ does not vanish and is given by

$$\gamma \approx 0.1176Pr^{-1} + 0.2058. \tag{A 8}$$

Again, it is easy to find concise approximations which are accurate to within a few percent. We have $\mu \approx \frac{5}{4}\pi$, $\bar{F} = 4(2+\sqrt{2})/5\pi$, $R_0\overline{G^2} = \frac{7}{3}\pi^2$ and $\overline{F'^2} = \frac{7}{6}\pi^2$. Using these approximations we have $\alpha \approx 16(14/3)^{\frac{1}{2}}/25\pi$ and from the definitions in (2.30)

$$\left.\begin{aligned} p \approx \tfrac{1}{4}(2+Pr^{-1}), \quad r \approx \frac{Ra-(\frac{5}{4}\pi)^4(1+\cos^2\theta)}{(14\pi^2/3)\,\epsilon^2}, \quad c \approx \frac{5(2+\sqrt{2})\,(3/14)^{\frac{1}{2}}\cos\theta}{4\epsilon}, \\ \beta \approx \frac{(\frac{3}{14})^{\frac{3}{2}}5(2+\sqrt{2})\sin(\theta-\theta')\,Ra}{4\pi^2\epsilon^3}. \end{aligned}\right\} \tag{A 9}$$

Appendix B. Linear stability boundaries

In this appendix we determine the linear stability boundaries shown in figure 3 for arbitrary values of θ. The linearized version of the non-dimensional, unforced equations of motion (2.10) is

$$\left.\begin{aligned} Pr^{-1}\epsilon^2(\epsilon^2\partial_x^2+\partial_z^2)\psi_t &= (\epsilon^2\partial_x^2+\partial_z^2)^2\psi-\sin\theta\, Ra\, b_z-\epsilon\cos\theta\, Ra\, b_x \\ \epsilon^2 b_t &= (\epsilon^2\partial_x^2+\partial_z^2)b-\sin\theta\psi_z-\epsilon\cos\theta\psi_x. \end{aligned}\right\} \tag{B 1}$$

Substituting $[\psi, b] = [\hat{\psi}(z), \hat{b}(z)]\exp(ikx+st)$ we obtain a system of ordinary differential equations for the vertical structure of the buoyancy and stream-function perturbations:

$$\left.\begin{aligned} \hat{\psi}^{\mathrm{iv}}-\epsilon^2(2k^2\hat{\psi}''+sPr^{-1}\hat{\psi})+\epsilon^4k^4\hat{\psi} &= Ra\sin\theta\hat{b}'+ik\epsilon\, Ra\cos\theta\hat{b}, \\ \hat{b}''-\epsilon^2(k^2+s)\hat{b} &= \sin\theta\hat{\psi}'+ik\epsilon\cos\theta\hat{\psi}. \end{aligned}\right\} \tag{B 2}$$

We expand $\hat{\psi}$, $\hat{b}$, and Ra in powers of ϵ, and to zeroth order in ϵ we obtain:

$$\psi_0^{\mathrm{iv}} = R_0\sin\theta b_0', \quad b_0'' = \sin\theta\psi_0'. \tag{B 3}$$

When we solve (B 3) for a slip boundary condition and $\psi = b_z = 0$ on $z = \pm\frac{1}{2}$ we find that there are two possibilities. One is

$$\psi_0 = \cos(\pi z), \quad b_0 = \pi^{-1}\sin\theta\sin(\pi z), \tag{B 4}$$

which implies that $R_0\sin^2\theta = \pi^4$. This critical Rayleigh number is shown as a dashed curve in figure 3. The other possibility is

$$\psi_0 = 0, \quad b_0 = 1 \tag{B 5}$$

and the critical Rayleigh number is determined at $O(\epsilon^2)$. The stream function is $O(\epsilon)$ and satisfies

$$\psi_1^{\mathrm{iv}}-R_0\sin^2\theta\psi_1 = ikR_0\cos\theta. \tag{B 6}$$

Defining $\lambda^4 \equiv R_0\sin^2\theta$ the stream function is

$$\psi_1 = -ik\frac{\cos\theta}{\sin^2\theta}\left[1-\frac{\cos(\lambda z)}{2\cos(\frac{1}{2}\lambda)}-\frac{\cosh(\lambda z)}{2\cosh(\frac{1}{2}\lambda)}\right], \quad b_1' = \sin\theta\psi_1. \tag{B 7}$$

In order to determine the critical Rayleigh number only the equation governing the time evolution of the buoyancy perturbation is needed at $O(\epsilon^2)$:

$$b_2''-\sin\theta\psi_2' = k^2+s+ik\cos\theta\psi_1. \tag{B 8}$$

Integrating (B 8) in z and making use of the boundary conditions and the result for ψ_1 we obtain

$$0 = s+k^2+k^2\cot^2\theta\left[1-\frac{\tan(\frac{1}{2}\lambda)}{\lambda}-\frac{\tanh(\frac{1}{2}\lambda)}{\lambda}\right]. \tag{B 9}$$

The stability boundary is obtained requiring that $s = 0$ and making use of the definition of λ terms of the Rayleigh number. The curve is shown in figure as dashed.

REFERENCES

CHANDRESAKHAR, S. 1961 *Hydrodynamic and Hydromagnetic Stability* Dover, 654+xix pp.

CHAPMAN, C. J., CHILDRESS, S. & PROCTOR, M. R. E. 1980 Long wavelength thermal convection between nonconducting boundaries. *Earth Planet. Sci. Lett.* **51**, 342–369.

CHAPMAN, C. J. & PROCTOR, M. R. E. 1980 Nonlinear Rayleigh–Bénard convection between poorly conducting boundaries. *J. Fluid Mech.* **101**, 759–782.

CHILDRESS, S. & SPIEGEL, E. A. 1992 Pattern formation in a suspension of swimming micro-organisms: nonlinear aspects. *J. Fluid Mech.* (submitted).

CORMACK, D. E., LEAL, L. G. & IMBERGER, J. 1974*a* Natural convection in a shallow cavity with differentially heated end walls. Part 1. Asymptotic theory. *J. Fluid Mech.* **65**, 209–229.

CORMACK, D. E., LEAL, L. G. & SEINFELD, J. H. 1974 Natural convection in a shallow cavity with differentially heated end walls. Part 2. Numerical solutions. *J. Fluid Mech.* **65**, 231–246.

DEPASSIER, M. C. & SPIEGEL, E. A. 1982 Convection with heat flux prescribed on the boundaries of the system. I. The effect of temperature dependence on material properties. *Geophys. Astrophys. Fluid Dyn.* **21**, 167–188.

ELDER, J. W. 1965 Laminar free convection in a vertical slot. *J. Fluid Mech.* **23**, 77–98.

IMBERGER, J. 1974 Natural convection in a shallow cavity with differentially heated end walls. Part 3. Experimental results. *J. Fluid Mech.* **65**, 247–260.

LINZ, S. 1990 Naturally driven dispersion in tilted porous layers. In *Proc. Woods Hole Oceanographic Inst. Summer Study Program in Geophysical Fluid Dynamics.*

NORMAND, C. 1984 Nonlinear convection in high vertical channels. *J. Fluid Mech.* **143**, 223–242.

PHILLIPS, O. M. 1970 On flows induced by diffusion in a stably stratified fluid. *Deep-Sea Res.* **17**, 435–443.

PROCTOR, M. R. E. & HOLYER, J. Y. 1986 Planform selection in salt fingers. *J. Fluid Mech.* **168**, 241–253.

RILEY, D. S. & WINTERS, K. H. 1990 A numerical bifurcation study of natural convection in a tilted two dimensional porous cavity. *J. Fluid Mech.* **215**, 309–329.

ROBERTS, A. J. 1985 An analysis of near-marginal, mildly penetrative convection with heat flux prescribed on the boundaries. *J. Fluid Mech.* **158**, 71–93.

SEN, M., VASSEUR, P. & ROBILLARD, L. 1988 Parallel flow convection in a tilted two-dimensional porous layer heated from all sides. *Phys. Fluids* **31**, 3480–3487.